ELSEVIER

CrossMark

The impact of aging, hearing loss, and body weight on mouse hippocampal redox state, measured in brain slices using fluorescence imaging

Kevin A. Stebbings [a], Hyun W. Choi [b], Aditya Ravindra [b], Daniel Adolfo Llano [a,b,*]

[a] *Neuroscience Program, University of Illinois at Urbana-Champaign, Urbana, Illinois, USA*
[b] *Department of Molecular and Integrative Physiology, University of Illinois at Urbana-Champaign, Urbana, Illinois, USA*

ARTICLE INFO

ABSTRACT

The relationships between oxidative stress in the hippocampus and other aging-related changes such as hearing loss, cortical thinning, or changes in body weight are not yet known. We measured the redox ratio in a number of neural structures in brain slices taken from young and aged mice. Hearing thresholds, body weight, and cortical thickness were also measured. We found striking aging-related increases in the redox ratio that were isolated to the stratum pyramidale, while such changes were not observed in thalamus or cortex. These changes were driven primarily by changes in flavin adenine dinucleotide, not nicotinamide adenine dinucleotide hydride. Multiple regression analysis suggested that neither hearing threshold nor cortical thickness independently contributed to this change in hippo-campal redox ratio. However, body weight did independently contribute to predicted changes in hip-pocampal redox ratio. These data suggest that aging-related changes in hippocampal redox ratio are not a general reflection of overall brain oxidative state but are highly localized, while still being related to at least one marker of late aging, weight loss at the end of life.

© 2016 Elsevier Inc. All rights reserved.

1. Background

Aging is associated with both cognitive changes and specific sensory changes, such as peripheral hearing loss. For example, aging-related deficits in episodic and spatial memory have been well documented in humans and animals (Albert, 1997; Buckner, 2004; Frick et al., 1995; Gallagher and Pelleymounter, 1988; Hedden and Gabrieli, 2004; Levine et al., 2002), as have changes in peripheral hearing function (Cruickshanks et al., 1998; Frisina and Zhu, 2010; Moscicki et al., 1985; Ohlemiller et al., 2010; Simpson et al., 1985; Syka, 2010). These changes in memory function are associated with changes in hippocampal structure and function that occur during aging (Driscoll et al., 2006; Golomb et al., 1994; Maguire and Frith, 2003; Persson et al., 2006), whereas the changes in auditory function are associated with loss of function at multiple levels of the auditory system, from the peripheral hearing apparatus to multiple levels of the central auditory system (Del Campo et al., 2012; Henry et al., 1980; Ling et al., 2005; Mendelson and Ricketts, 2001; Parthasarathy et al., 2010; Walton

et al., 1998). In addition, hearing loss and cognitive loss during aging are correlated (Lin et al., 2011a, 2011b), suggesting a potential common underlying etiology. It is not yet known whether changes in peripheral hearing are related in a direct and causal way to changes in general cognitive function, or if both are reflections of general metabolic factors, such as oxidative stress, which occur during aging (Beal, 1995; Berlett and Stadtman, 1997; Dröge and Schipper, 2007). Therefore, the goal of this study is to examine the relationships between aging, peripheral hearing loss, and oxidative stress in the hippocampus in an animal model.

Multiple approaches have been used to measure oxidative stress in the brain. Previous investigators have measured redox state via direct measurements of oxygen consumption in homogenized tissues (Kudin et al., 2002; Lores-Arnaiz et al., 2005). Potential limitations to this direct respirometric approach are the lack of spatial resolution of the sampling of the tissue, and the subsequent inability to conduct other experiments on the same tissue. Another approach to quantify redox state in brain tissue is to measure the ratio of oxidized flavin adenine dinucleotide (FAD) to reduced nicotinamide adenine dinucleotide hydride (NADH). FAD can be quantified by measuring the emitted fluorescence in tissue at approximately 525 nm after excitation with wavelengths of approximately 450–480 nm (Benson et al., 1979; Huang et al., 2002; Kunz and Gellerich, 1993). Cellular NADH can be quantified

* Corresponding author at: Neuroscience Program, University of Illinois at Urbana-Champaign, 2355 Beckman Institute, 405 North Mathews Avenue, Urbana, Illinois, 61801-2325, USA. Tel.: (217) 244-0740; fax: (217) 333-1133.
E-mail address: d-llano@illinois.edu (D.A. Llano).

by measuring the emitted fluorescence in tissue at approximately 450 nm after excitation with wavelengths of approximately 350 nm (Duchen et al., 2003; White and Wittenberg, 1993). Many investigators have used this ratio to measure oxidative stress across multiple tissue types, including brain (Gerich, et al., 2006, 2009; Maleki et al., 2012; Mayevsky, 1984; Parihar et al., 2008; Ranji et al., 2009), and this ratio has been established to be directly associated with tissue oxidative stress (Crowley et al., 2016; Salehpour et al., 2015). We and others found that this ratio can be measured in acutely prepared brain slices and is sensitive to small perturbations of molecules known to cause oxidative stress, such as hydrogen peroxide and cyanide (Gerich, et al., 2006, 2009; Stebbings et al., 2016). Consequently, using a standardized approach to cut brain slices that are similar animal-to-animal (validated by using electrical stimulation to establish synaptic connectivity), we can use the slice preparation to compare the redox state, measured as a ratio of FAD/NADH, in various brain subregions of the slices in a nondestructive way with high spatial resolution.

Therefore, in the present study, we measured the redox ratio of various hippocampal subfields, 2 auditory forebrain structures (auditory cortex [AC] and medial geniculate body [MGB]), as well as peripheral hearing thresholds in young and aged mice. This was done in brain slices taken from CBA/CaJ mice, which are known to undergo aging-related hearing loss, and loss of auditory efferent function (Frisina and Zhu, 2010; Frisina et al., 2011; Ohlemiller et al., 2010). In addition, body weight, which has a complex and age-dependent relationship with general health and longevity (Anisimov et al., 2004; Goodrick et al., 1990; Samorajski et al., 1985), was also measured. These data were obtained as part of a study of aging-related changes in inhibitory synaptic function in the AC whose results were already published (Stebbings et al., 2016).

2. Methods

2.1. Mice

A total of 29 male CBA/CaJ mice, obtained through the National Institute on Aging aged rodent colonies, were used in these studies. The young group comprised 16 animals: 5 at 4 months, 5 at 5.5 months, 5 at 9 months, and 1 at 13 months of age. The aged group comprised 13 animals: 4 at 20 months, 5 at 22 months, 3 at 23 months, and 1 at 28.4 months. Body weight was measured in 22 animals. Other measures of general metabolic health were not assessed. All procedures were approved by the Institutional Animal Care and Use Committee at the University of Illinois. All animals were housed in animal care facilities approved by the American Association for Assessment and Accreditation of Laboratory Animal Care.

2.2. Auditory brainstem responses

As previously described (Stebbings et al., 2016), ABRs were obtained at frequencies of 4, 8, 16, 32, 45, and 64 kHz as well as broadband noise. It was not possible to obtain all frequencies for all animals. Animals were anesthetized with 100 mg/kg ketamine + 3 mg/kg xylazine intraperitoneally before the insertion of 2 subdermal electrodes, 1 at the vertex and 1 behind the left ear. Stimuli were presented using a Tucker-Davis Technologies system 3, ES1 free field speaker, with waveforms being generated by RPvdsEx software. The output of the Tucker-Davis Technologies speaker was calibrated at all the relevant frequencies, using a Bruel and Kjaer type 4135 microphone and a Bruel and Kjaer measuring amplifier (Model 2610). Each frequency was presented for 5 ms (3 ms flat with 1 ms for both rise and fall times) at a rate of 2–6 Hz, varied

within each animal, with a 100 ms analysis window. Raw potentials were obtained with a Dagan 2400A amplifier and preamplifier headstage combination, and filtered between 100 Hz and 3000 Hz. An AD instruments power lab 4/30 system was used to average these waveforms 500 times. Significant deflections, assessed via visual inspection, within 10 ms after the end of the stimulus were deemed a response. Hearing threshold in response to a noise stimulus was chosen as the main hearing metric because all animals had a measurable ABR response to noise and because a principal components analysis showed that noise thresholds were essentially interchangeable with virtually any combination of pure-tone thresholds or thresholds averaged across frequencies (data not shown). Initial attempts were made to do the ABRs blinded, as we have done previously (Llano et al., 2012). However, we found this to be impossible given the physical differences between the young and aged mice (i.e., aged mice were larger and had substantially less whiskers on their snouts). Given the large differences seen in the ABR thresholds seen in a larger data set using these same animals (19 dB difference, $p < 0.0001$; Stebbings et al., 2016), it is unlikely that functional unblinding played a role in the differences reported here.

2.3. Brain slicing

As previously described (Stebbings et al., 2016), we modified the thalamocortical brain slice preparation developed by Cruikshank et al. (2002) to increase the likelihood of retaining the lateral extent of thalamocortical afferents to the left AC. To ensure maximum slice viability, mice were initially anesthetized with ketamine (100 mg/kg) + xylazine (3 mg/kg) intraperitoneally and perfused with chilled (4 °C) sucrose-based slicing solution (in mM): 234 sucrose, 11 glucose, 26 $NaHCO_3$, 2.5 KCl, 1.25 NaH_2PO_4, 10 $MgCl_2$, 0.5 $CaCl_2$. Brains were blocked by removing of the olfactory bulbs and the anterior 2 mm of frontal cortex with a razor blade. The brain was then tipped onto the coronal cut and an off-horizontal cut was made on the dorsal surface, removing a sliver of brain angled at 20° from the horizontal plane. This increase in cutting angle of the thalamocortical slice has also been used previously in older gerbils (Takesian et al., 2012). The brain was then glued onto the cut angled surface, and 600 μm thick sections were taken. Sections were incubated for 1 hour in 32 °C incubation solution before being imaged (26 $NaHCO_3$, 2.5 KCl, 10 glucose, 126 NaCl, 1.25 NaH_2PO_4, 3 $MgCl_2$, and 1 $CaCl_2$). After incubation, slices were transferred to a chamber with an elevated slice platform so that the tissue could be perfused from both above and below with artificial cerebrospinal fluid (26 $NaHCO_3$, 2.5 KCl, 10 glucose, 126 NaCl, 1.25 NaH_2PO_4, 2 $MgCl_2$, and 2 $CaCl_2$, 22 °C and bubbled with 95% oxygen/5% carbon dioxide).

Endogenous flavoprotein (FAD) autofluorescence was measured using a stable DC fluorescence illuminator (Prior Lumen 200) and a U-M49002Xl E-GFP Olympus filter cube (excitation: 470–490 nm, dichroic 505 nm, emission 515 nm long pass). Endogenous NADH imaging was performed using a Semrock Sirius A 000 cube with 350–390 nm excitation and 415–465 nm emission. Redox ratios were expressed as a ratio of FAD to NADH (Sepehr et al., 2012). All data were collected using an infinity corrected Olympus MacroXL 4X objective (NA 0.28) and a Retiga EXi camera using 4 × 4 binning (with resulting image size of 348 × 260 pixels) and StreamPix software.

2.4. Analysis

Regions of interest (ROI) in the hippocampus were defined anatomically by visualization of CA1, CA2, and CA3 in the slice. Initial hippocampal ROIs were 2 × 10 or 2 × 12 pixel rectangles

completely contained within the stratum pyramidale or stratum radiatum, respectively, in each hippocampal subfield (see Fig. 1A). Once it was determined that the most conspicuous changes were seen in CA2 and CA3, a new ROI containing these fields was constructed (see Fig. 1B). The ROI in the dentate gyrus (DG) was drawn analogously to the ROIs in CA1, CA2, and CA3. The MGB ROI was constructed using a 20×40 pixel rectangle totally contained within the MGB. The AC ROI corresponds to a 2 mm rostrocaudal region centered around the area of activation seen after stimulation of auditory thalamocortical afferents, done as part of a previous study with the same slices (Stebbings et al., 2016). All pixels in each ROI were averaged in the calculation of redox ratios. Cortical thickness was evaluated by drawing a line tangent to the rostral-most extent of the hippocampus, from the white and/or gray matter border of the cortex to the pia.

2.5. Statistics

Given the nonuniform distribution of ages in the study (mostly young or aged animals, with few in between), nonparametric statistics (2-tailed Wilcoxon-Rank Sum test and Spearman's correlation) were used. For multivariate comparisons, multiple linear regression (run in SPSS) was used to test relative contributions of age, hearing loss, cortical thickness, and body weight on hippocampal redox ratios. An optimal multivariate model was chosen by including all combinations of age, hearing, cortical thickness, and body weight as independent variables and computing the adjusted R^2 values. Regression coefficients and p-values were then computed using the optimal model. Wald chi-squared testing was run in SAS to test for interaction effects. Correction for multiple comparisons was done using the Holm-Bonferroni method (Holm, 1979).

3. Results

Fig. 2 shows representative images from brain slices taken from animals ranging from 4 months to 28.4 months of age. Shown are FAD images (Fig. 2A–D), NADH images (Fig. 2E–H), and images of the redox ratio (Fig. 2I–L). These exemplar data indicate that there is a progressive increase in the FAD signal and redox ratio seen with aging which is most conspicuous in the stratum pyramidale of the

hippocampus, particularly in the CA2 and CA3 regions (denoted by arrows in Fig. 2L).

We examined the relationship between age and redox ratio across multiple brain structures. Fig. 1A illustrates the ROI for the AC, MGB, hippocampus CA1, CA2, and CA3 regions (both for the stratum pyramidale and adjacent stratum radiatum). Fig. 1B shows a modified ROI containing a large strip extending from the CA1/CA2 border, through all of visible CA3, in both the stratum pyramidale and adjacent stratum radiatum. As will be shown below, these were the areas containing the most conspicuous aging-related changes and were therefore used for all subsequent analyses.

Fig. 3A shows the redox ratios of each of these brain structures (AC, MGB, CA1, CA2, and CA3) for both young and aged animals. There are no significant differences between young and aged in the DG, MGB, or AC. There is an aging-related increase in the redox ratio in CA2 (young $= 0.56 \pm 0.08$ vs. aged $= 0.65 \pm 0.08$, $p = 0.007$) and a trend for significance in CA3 (young $= 0.55 \pm 0.07$ vs. aged $= 0.64 \pm 0.08$, $p = 0.021$) which did not survive correction for multiple comparisons.

To achieve a more standardized measurement that would be less sensitive to differences in slice preparation, the redox ratio in the stratum pyramidale of the hippocampal subfields was normalized to the redox ratio in the stratum radiatum. These normalized redox ratios are shown in Fig. 3B. As shown, there were significant increases in the normalized redox ratio seen with aging in all subfields, and pairwise comparisons (young vs. aged) showed that this increase was most highly significant ($p < 0.0001$) in CA2 and CA3 subfields. We therefore used this ratio from a combined CA2 + CA3 ROI for all subsequent analyses and refer to this is as the "CA2-CA3 normalized redox ratio." Note that we have also used the normalized redox ratio of either CA2 or CA3 and a combined CA1-CA2-CA3 ROI as a dependent variable, and we have found no substantial differences from analysis with the CA2-CA3 normalized redox. The trends for CA1 ratio were generally in the same direction as CA2 and CA3, but weaker and are not analyzed further (data not shown).

To determine if the increase in redox ratio was driven by a change in FAD or NADH, or both, we have separately analyzed aging-related changes in the FAD and NADH signal. Because FAD and NADH measurements were not standardized (i.e., different exposure times were used in each slice and were optimized for each slice), the ratio of each component in the stratum pyramidale was
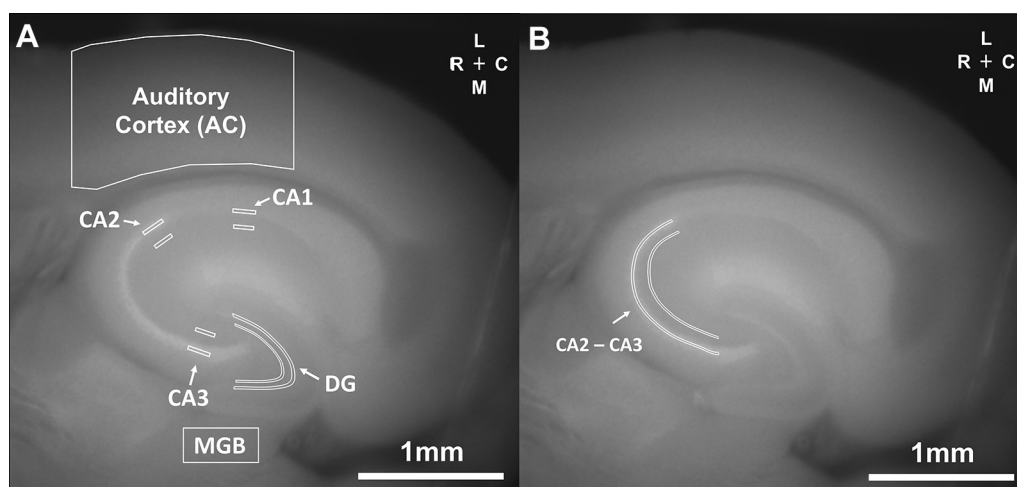

Fig. 1. ROIs used in this study. (A) The original ROIs used were those from the AC and MGB, as well as the stratum pyramidale and adjacent stratum radiatum in regions CA1, CA2, and CA3. (B) Once it was determined that the largest aging-related signal changes were seen in CA2 and CA3, a new region of interest capturing the stratum pyramidale and stratum radiatum of both of CA2 and CA3 was used for subsequent analyses. Abbreviations: DG, dentate gyrus; MGB, medial geniculate body; NADH, nicotinamide adenine dinucleotide hydride; ROI, regions of interest.
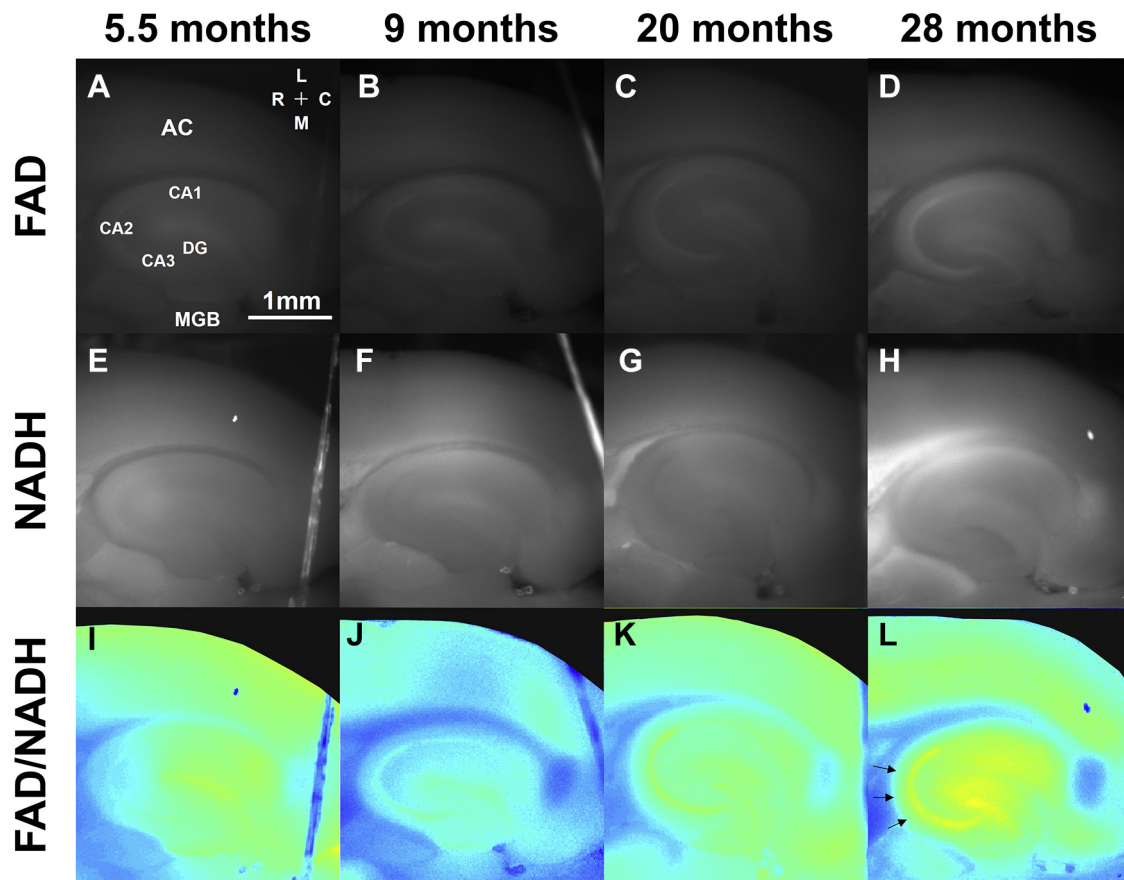
5.5 months   9 months   20 months   28 months

Fig. 2. Representative examples of FAD images (A–D), NADH images (E–H), and redox ratio images (I–L) from mice taken from different age groups. The notable finding in this figure is the rise of the FAD signal and redox ratio observed in the stratum pyramidale of the hippocampus (see arrows in L). Abbreviations: AC, auditory cortex; DG, dentate gyrus; FAD, flavin adenine dinucleotide; MGB, medial geniculate body; NADH, nicotinamide adenine dinucleotide hydride.

normalized to the value measured in the stratum radiatum. We observed a highly significant relationship between age and the FAD ratio obtained using the combined ROI encompassing CA2 and CA3 (Spearman's rho = 0.823, $p < 0.0001$, degrees of freedom [DF] = 27), but no significant relationship for NADH (Spearman's rho = 0.098, $p < 0.61$, DF = 27). These data suggest that the aging-dependent rise in the redox ratio is driven by the FAD component of the signal, not the NADH component.

Multiple other end points also show aging-dependent changes in mice, such as hearing threshold, cortical thickness, and body weight (Frisina and Zhu, 2010; Frisina et al., 2011; Goodrick et al., 1990; Ohlemiller et al., 2010; Samorajski et al., 1985; Stebbings et al., 2016). Therefore, we examined whether any of these factors were associated with hippocampal redox signal changes. Fig. 4A–D shows the individual correlation functions between each of these factors and the CA2-CA3 normalized redox ratio. As shown, age, cortical thickness, and hearing threshold are strongly correlated with CA2-CA3 normalized redox ratio ($p < 0.001$ in all cases), while body weight is not ($p = 0.636$). Note in Fig. 4C that the normalized redox ratio appears to asymptote at approximately 1.1 at hearing thresholds above 50 dB sound pressure level and is better fit by a logarithmic function (R = 0.695).

Given the multiple potential predictors of the CA2-CA3 normalized redox ratio shown in Fig. 4, we attempted to separate out the effect of each one using multiple regression. Standard multiple linear regression was done to determine if cortical thickness, hearing threshold, or body weight independently contributed to aging-related changes in the CA2-CA3 normalized redox ratio. All

combinations of age, cortical thickness, hearing threshold, and body weight were used nonsequentially to develop an optimal model based on adjusted R^2 values. The largest adjusted R^2 value was found when combining age and body weight (adjusted $R^2 = 0.855$). For this model, both age (standardized beta = 1.003, $p < 0.001$) and body weight (standardized beta = −0.254, $p = 0.011$) were significant independent predictors of CA2-CA3 normalized redox ratio (Table 1). Variance inflation factors (VIFs) were computed for each of these factors and were found to be low (VIFs = 1.19), suggesting little collinearity between these variables (O'Brien, 2007).

To further explore the relationships between hearing loss, body weight, aging, and CA2-CA3 normalized redox ratio, we plotted body weight versus hearing loss and body weight versus CA2-CA3 normalized redox ratio, and analyzed these separately for young and aged animals. Fig. 5A shows such a plot for hearing loss. As shown, the regression slope for body weight versus hearing loss is essentially flat in the young animals ($p = 0.34$), but a strong correlation between body weight and hearing loss exists in the aged animals ($p = 0.0005$). That is, older, lighter animals had the most significant hearing loss, whereas older, heavier animals had hearing thresholds similar to young animals. Similar interactions were seen for CA2-CA3 redox ratio (Fig. 5B). As was the case for hearing loss, the correlation function for body weight versus hearing loss is essentially flat in the young animals ($p = 0.78$) but shows a strong correlation in the aged animals ($p = 0.003$). Although it is possible the lack of significant correlations observed with the young animals is related to type II error, the slopes of the regression lines are essentially flat, suggesting weak, if any, relationships between these
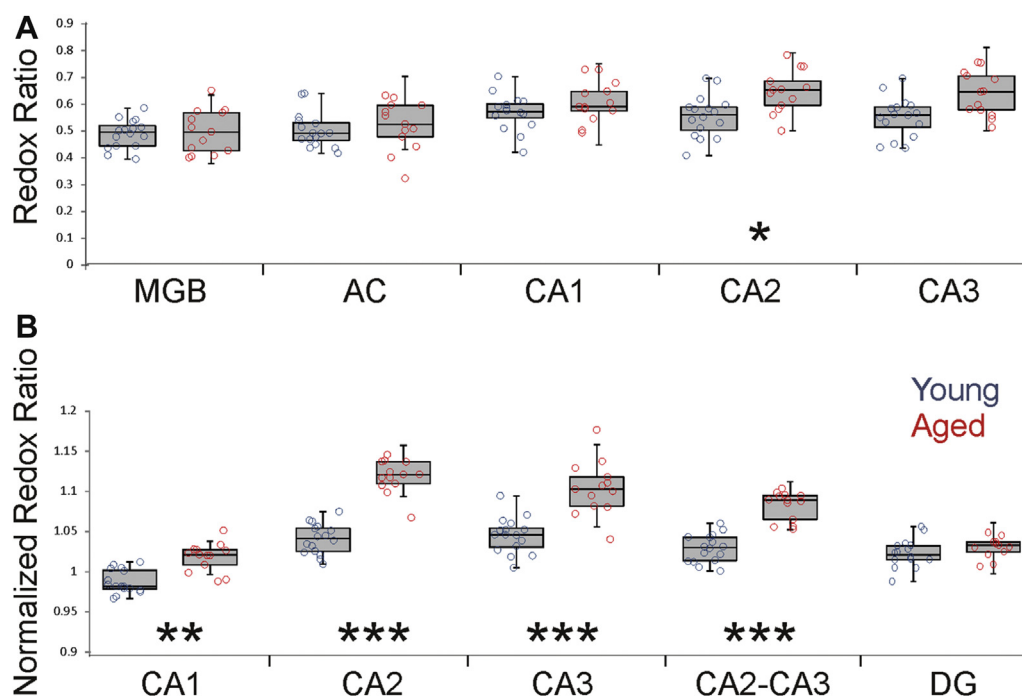
Fig. 3. (A) Box-whisker plots showing median, quartiles 1 and 3, minimum and maximum values overlaid on scatterplots of the individual values of the redox ratio across 5 different brain regions in young (blue) and aged (red) mice. Significance for each region is as follows: AC: $p = 0.369$, U = 83; MGB: $p = 0.913$, U = 101; CA1: $p = 0.228$, U = 76; CA2: $p = 0.007$, U = 41; CA3: $p = 0.021$, U = 51. In all cases, DF = 27. (B) Box and whisker plots of normalized redox ratios from CA1, CA2, CA3, a combined ROI containing both CA2 and CA3 and the DG significance for each region is as follows: CA1: $p = 0.0001$, U = 17.0; CA2: $p < 0.0001$, U = 1; CA3: $p < 0.0001$, U = 13; CA2-CA3: $p < 0.0001$, U = 3; DG: $p = 0.101$, U = 66. In all cases, DF = 27. $^*p < 0.01$, $^{**}p < 0.001$, $^{***}p < 0.0001$. Abbreviations: AC, auditory cortex; DF, degrees of freedom; DG, dentate gyrus; MGB, medial geniculate body; ROI, regions of interest.

variables. Note that none of the aging- and body weight-related findings can be explained by correlations between age and weight, since these are uncorrelated in both the whole population (Spearman's rho = 0.353, $p = 0.11$, DF = 20), as well as the aged animals (Spearman's rho = −0.361, $p = 0.25$, DF = 10).

These data suggest the presence of interaction effects between age, body weight, and hippocampal redox ratio. That is, older, lighter animals had the highest hippocampal redox ratios, whereas older, heavier animals had hippocampal redox ratios approaching those of young animals. Interaction effects were examined in both cases using the Wald chi-square test. In both cases, it was determined that body weight significantly affected aging-related changes in hearing loss and CA2-CA3 normalized redox ratio, though the interaction was stronger with hearing loss ($p < 0.0001$, chi-square = 23.7) than CA2-CA3 normalized redox ratio ($p = 0.037$, chi-square = 4.4).

Given the interactions between body weight, age, and normalized CA2-CA3 redox ratios described in the previous paragraph, we used multiple linear regression to examine the contribution of body weight, but now only in the aged animals. As was done in the previous paragraph, all permutations of age, cortical thickness, hearing threshold, and body weight were used to develop an optimal model based on adjusted R^2 values. The largest adjusted R^2 value was found when combining age, hearing loss, and body weight (adjusted $R^2 = 0.502$). However, VIFs for this model were somewhat elevated for weight (VIF = 5.62) and noise threshold (VIF = 5.74). Therefore, we estimated the VIFs for the model with the second highest R^2 value (i.e., the model containing age and body weight) and found the VIFs to be in a more acceptable range (VIFs = 1.10). For this model, adjusted $R^2 = 0.472$, and only body weight ($p = 0.011$) was a significant independent predictor of CA2-CA3 normalized redox ratio (Table 1).

4. Discussion

In the present study, we report aging-related changes in the redox ratio (FAD/NADH) of the CA subfields of the hippocampus using fluorescence imaging of intrinsic FAD and NADH signals from slices taken from the CBA/CaJ mouse. These redox changes were almost totally driven by changes in the relative intensity of the FAD signal, were less prominent in CA1, and were not seen in the DG, AC, or the MGB. The normalized CA2-CA3 redox ratio also correlated positively with hearing loss and inversely with cortical thickness, though neither of these contributed significantly to this ratio beyond the contribution of aging. Body weight was found to independently contribute to the normalized CA2-CA3 redox changes; particularly so in the aging animals. These data are consistent with a body of literature demonstrating selective aging-related vulnerability to oxidative stress in the hippocampus, suggesting that peripheral hearing loss and hippocampal redox changes may share common mechanisms, and point to the possibility of using body weight as a window into the oxidative state of hippocampal neurons.

4.1. Methodological considerations

The process of perfusing a mouse and cutting brain slices almost certainly introduces significant metabolic stress in brain tissue, and, in fact, we have previously shown that certain portions of the slice do not survive this trauma (Llano et al., 2014). In addition, there have been numerous previous studies demonstrating that the aging brain, particularly the hippocampus, is highly sensitive to metabolic insults (El Mohsen et al., 2005; Huang et al., 2015; Navarro et al., 2008; Parihar et al., 2008; Siqueira et al., 2005). Therefore, it is possible that the aging-related differences in the CA2 and CA3
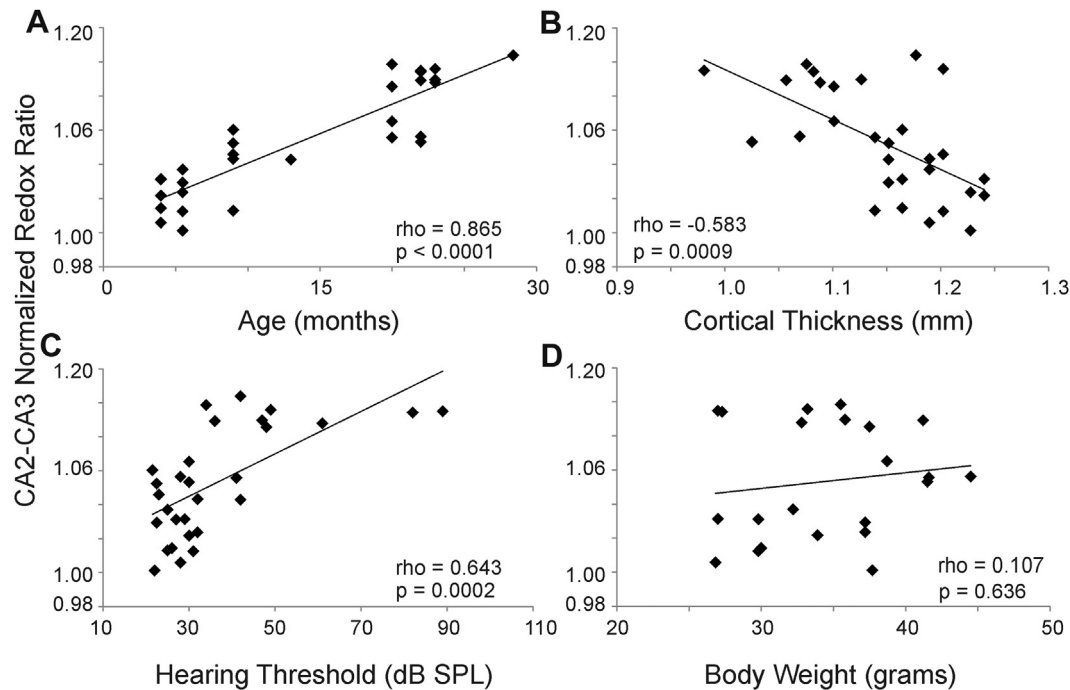
Fig. 4. Correlation functions for (A) age, (B) cortical thickness, (C) hearing threshold, and (D) body weight, all versus CA2-CA3 normalized redox ratio. Correlation coefficients were determined using Spearman's correlation and denoted as rho. DF = 27 for panels A–C. DF = 20 for panel D. Abbreviation: DF, degrees of freedom.

redox state seen in the present study are driven by the metabolic stress induced by the production of brain slices and may not reflect differences that would be seen in situ in a living organism. The finding that the aging-related increase in redox ratio is isolated to a particular layer of the hippocampus suggests that, at the very least, our results are not related to global metabolic stress on tissue caused by the slicing process. However, it is possible that our results are the result of some combination of intrinsic differences in the redox state of CA2 and CA3 neurons, and redox changes in selectively vulnerable neurons that were induced by the slicing process. This question could be answered with the development of a method to provide high-resolution redox imaging of deep tissues in vivo, which, to our knowledge, is not yet possible.

Another methodological consideration is that the cellular source of the FAD and NADH signals observed in this study are not yet known. It has been speculated that most of the FAD signal seen in the brain is from neuronal, rather than glial, origin (Husson and Issa, 2009). This is because, at least in the primate visual cortex, it has been shown that approximately 2% of the mitochondria are found in glia, and the rest are found in dendrites (Wong-Riley, 1989). However, other work has demonstrated that at least part of the FAD signal seen in vivo in the cerebellar cortex after electrical stimulation is of glial origin (Reinert et al., 2007). Neither of these studies examined the potential glial contribution to FAD or NADH

autofluoresence signals in the hippocampus. Therefore, the potential contribution of cell type to the current results remains unknown.

Finally, as a correlative study, no specific interventions were done in the current work to determine if causal relationships exist between any of the measured variables. For example, in future work, it would be interesting to specifically induce hearing loss or body weight changes in an experimental animal and ask if either of these two alter hippocampal redox ratios.

4.2. Implications for hippocampal function and aging

The current data add to a growing body of literature demonstrating aging-related increases in mitochondrial dysfunction and that this dysfunction is particularly notable in the hippocampus (El Mohsen et al., 2005; Huang et al., 2015; Navarro et al., 2008; Parihar and Brewer, 2007; Parihar et al., 2008; Siqueira et al., 2005). One difference between our work and at least one other study is that the aging-related changes in the present study appear to be driven by a rise in the FAD signal, rather than changes in the NADH signal seen in cultured hippocampal neurons (Parihar et al., 2008). The differences between our findings and those of previous investigators may be related to the different approaches used. As mentioned in the previous paragraphs, it is likely that each method used to measure oxidative stress in brain tissue (brain slicing, cell culture, tissue homogenization), introduces new metabolic insults which may be reflected in the redox state of the tissue.

Peripheral hearing loss is strongly epidemiologically linked to aging-related cognitive changes (Lin et al., 2011a, 2011b) and, consistent with this finding, the current data also suggest that hearing loss is correlated with hippocampal redox changes. The present data provide no additional evidence that natural hearing loss (presbycusis), which is highly correlated with age, contributes independently to redox changes. This stands in potential contrast with previous studies demonstrating that direct induction of

Table 1
Regression coefficients (standardized) and *p*-values from optimal multiple regression models including age and body weight as regressors

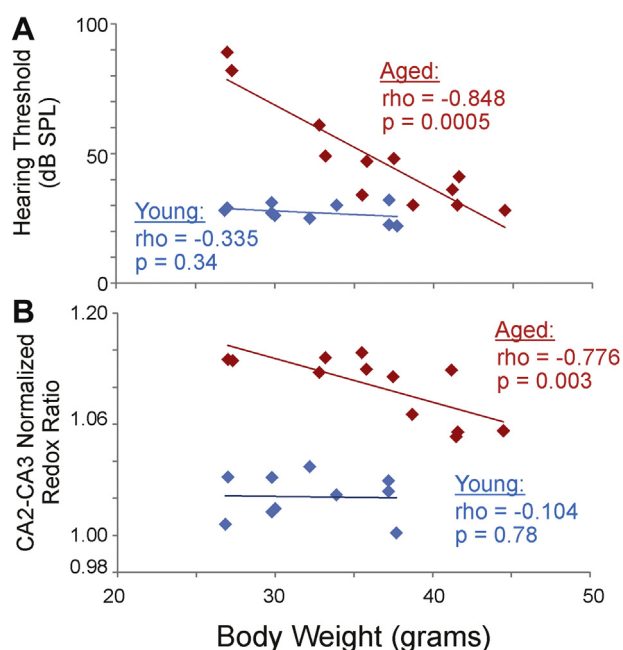| Factor	Beta	*p*-value
All animals (n = 22)		
Age	1.003	<0.001
Body weight	−0.254	0.011
Aged animals (n = 12)		
Age	0.054	0.820
Body weight	−0.736	0.011

Fig. 5. Correlation functions for (A) body weight versus hearing loss and (B) body weight versus CA2-CA3 normalized redox ratio, analyzed separately for young (blue) and aged (red) mice. (B) Same figure as Fig. 4D, except that young and aged mice are separated by color. Correlation coefficients were determined using Spearman's correlation and denoted as rho. DF = 10 for aged and 8 for young. Abbreviation: DF, degrees of freedom.

acoustic trauma using noise stimuli also produces general cognitive changes in experimental animals (Cernak et al., 2001; Cui et al., 2012). It is important to note in this context that the relationship, if any, between the redox changes seen in CA2 and CA3 in the present study, and cognitive performance, is not yet known. The alternative hypothesis, that hearing loss and hippocampal changes share a common metabolic etiology, is more consistent with current data and other previous work. Recent studies have demonstrated increases in markers of metabolic stress in the peripheral hearing apparatus seen during presbycusis (Jiang et al., 2007; Yamasoba et al., 2007). These data suggest that aging is associated with metabolic stress, which impacts both the peripheral hearing apparatus and the hippocampus. In the present study, we observed that body weight is inversely correlated with hearing loss and with CA2-CA3 redox ratio, but only in the aged animals (Fig. 5). This finding was unexpected, given the body of literature demonstrating cognitive, hearing, and lifespan benefits of caloric restriction (Sohal and Weindruch, 1996; Someya et al., 2007). Under normal conditions, body weight increases with age in mice, but then drifts downward at the oldest ages (Goodrick et al., 1990; Miller et al., 2002; Piantanelli et al., 2001; Samorajski et al., 1985). Although lower body weights at mid-life may predict better late-life health outcomes in rodents, this relationship weakens for body weights measured once animals are senescent (Miller et al., 2002; Piantanelli et al., 2001) and shows variability based on strain and specific health outcomes measured (Anisimov et al., 2004). Therefore, one potential explanation of these data is that older, lighter animals may be generally less healthy, manifesting in lowered body weight, worsened hearing, and higher hippocampal redox ratios. Alternatively, it is possible that lowered body weight represents a compensatory mechanism on the part of the animal to counteract neural and hearing dysfunction by diminishing caloric intake. Further studies involving measurements of other determinants of metabolic health and calorie consumption or studies using

induction of caloric restriction and observation of changes in redox ratio and hearing function correlations will help to answer these questions.

The mechanism(s) underlying the aging-related elevation of the FAD/NADH ratio in the stratum pyramidale of the CA portions of the hippocampus are not yet known. The hippocampus is home to multiple forms of synaptic plasticity which may involve elevations of intracellular calcium and the necessary production of reactive oxygen species (ROS), placing hippocampal neurons at general risk for oxidative stress (Hu et al., 2006; Paula-Lima et al., 2014). Intrinsic ROS-scavenging defenses undergo changes over the lifespan (Serrano and Klann, 2004), leaving the hippocampus more vulnerable to ROS during aging (El Mohsen et al., 2005; Rodrigues Siqueira et al., 2005). The hippocampus also displays aging-related changes in the production of enzymes needed for oxidative phosphorylation. The main enzymes involved in activity-dependent FAD oxidation (and therefore increase in FAD fluorescence) are the pyruvate decarboxylase complex and the enzymes of complexes I and II of oxidative phosphorylation (Husson and Issa, 2009). The stratum pyramidale of the hippocampus, in particular, expresses high levels of complex I enzymes (Manczak et al., 2005); however, these enzymes also undergo complex aging-related changes (Navarro et al., 2008), with one group of investigators suggesting that aging-related increases in complex I activity may be compensatory (Manczak et al., 2005). These data suggest that the aging-related elevations seen in the FAD signal could be a consequence of these compensatory increases, although one would also expect there to be a concomitant drop in the NADH signal, given the role of complex I in oxidizing NADH. Alternatively, rather than a compensatory response, a tonic shift in the redox potential may be driven by aging-related mitochondrial dysfunction and an increased supply of ROS. Such a shift in redox potential would lead to a larger proportion of $FADH_2$ and NADH molecules to exist in their oxidized forms, leading to an increase in the FAD/NADH ratio in tissues most sensitive to oxidative stress. Such vulnerable tissues would include hippocampal neurons, as described previously, and cells in the peripheral hearing apparatus, whose dysfunction would lead to hearing loss (Jiang et al., 2007; Poirrier et al., 2010; Staecker et al., 2001). This hypothesis would be consistent with our observations that hearing loss is correlated to hippocampal redox changes with aging (Fig. 4C). Neither explanation adequately accounts for the absence in NADH signal change with aging, unless changes in NADH fluorescence are an insensitive marker compared to FAD. To our knowledge, this has not been studied systematically. However, we have previously observed that FAD signal changes are substantially larger than NADH signal changes when being used as a surrogate marker for neural activity (Llano et al., 2014).

4.3. Conclusions

The current data extend previous work demonstrating aging-related changes in the redox state of the hippocampus. This increased vulnerability of the hippocampus relative to other brain structures may be responsible for the early aging-related losses in hippocampal volume, loss of episodic memory, and susceptibility to neurotoxic insults, such as to glutamate or amyloid beta, the agent found to be widely deposited in the brain in Alzheimer disease (Brewer et al., 2010). Furthermore, the present studies represent an additional approach to measure quantitative hippocampal redox ratio in living tissue with major portions of hippocampal circuitry retained. This approach may permit future studies that examine the relationship between aging, hippocampal redox state, and the function of neural circuits within the hippocampus.

Disclosure statement

The authors have no conflicts of interest to disclose.

Acknowledgements

References

Albert, M.S., 1997. The ageing brain: normal and abnormal memory. Philos. Trans. R. Soc. Lond. B Biol. Sci. 352, 1703–1709.

Anisimov, V.N., Arbeev, K.G., Popovich, I.G., Zabezhinksi, M.A., Rosenfeld, S.V., Piskunova, T.S., Arbeeva, L.S., Semenchenko, A.V., Yashin, A.I., 2004. Body weight is not always a good predictor of longevity in mice. Exp. Gerontol. 39, 305–319.

Beal, M.F., 1995. Aging, energy, and oxidative stress in neurodegenerative diseases. Ann. Neurol. 38, 357–366.

Benson, R.C., Meyer, R.A., Zaruba, M.E., McKhann, G.M., 1979. Cellular autofluorescence—is it due to flavins? J. Histochem. Cytochem. 27, 44–48.

Berlett, B.S., Stadtman, E.R., 1997. Protein oxidation in aging, disease, and oxidative stress. J. Biol. Chem. 272, 20313–20316.

Brewer, G.J., Torricelli, J.R., Lindsey, A.L., Kunz, E.Z., Neuman, A., Fisher, D.R., Joseph, J.A., 2010. Age-related toxicity of amyloid-beta associated with increased pERK and pCREB in primary hippocampal neurons: reversal by blueberry extract. J. Nutr. Biochem. 21, 991–998.

Buckner, R.L., 2004. Memory and executive function in aging and AD: multiple factors that cause decline and reserve factors that compensate. Neuron 44, 195–208.

Cernak, I., Wang, Z., Jiang, J., Bian, X., Savic, J., 2001. Cognitive deficits following blast injury-induced neurotrauma: possible involvement of nitric oxide. Brain Inj. 15, 593–612.

Crowley, A., Yang, C., Zheleznova, N.N., Staruschenko, A., Kurth, T., Rein, L., Sadovnikov, V., Dayton, A., Hoffman, M., Ryan, R.P., Skelton, M.M., Salehpour, F., Ranji, M., Geurts, A., 2016. Evidence of the importance of Nox4 in production of hypertension in Dahl salt-sensitive rats. Hypertension 67, 440–450.

Cruickshanks, K.J., Wiley, T.L., Tweed, T.S., Klein, B.E., Klein, R., Mares-Perlman, J.A., Nondahl, D.M., 1998. Prevalence of hearing loss in older adults in Beaver Dam, Wisconsin the epidemiology of hearing loss study. Am. J. Epidemiol. 148, 879–886.

Cruikshank, S.J., Rose, H.J., Metherate, R., 2002. Auditory thalamocortical synaptic transmission in vitro. J. Neurophysiol. 87, 361–384.

Cui, B., Wu, M., She, X., Liu, H., 2012. Impulse noise exposure in rats causes cognitive deficits and changes in hippocampal neurotransmitter signaling and tau phosphorylation. Brain Res. 1427, 35–43.

Del Campo, H.M., Measor, K., Razak, K., 2012. Parvalbumin immunoreactivity in the auditory cortex of a mouse model of presbycusis. Hear. Res. 294, 31–39.

Driscoll, I., Howard, S., Stone, J., Monfils, M., Tomanek, B., Brooks, W., Sutherland, R., 2006. The aging hippocampus: a multi-level analysis in the rat. Neuroscience 139, 1173–1185.

Dröge, W., Schipper, H.M., 2007. Oxidative stress and aberrant signaling in aging and cognitive decline. Aging Cell 6, 361–370.

Duchen, M.R., Surin, A., Jacobson, J., 2003. [17] Imaging mitochondrial function in intact cells. Methods Enzymol 361, 353–389.

El Mohsen, M.M.A., Iravani, M.M., Spencer, J.P., Rose, S., Fahim, A.T., Motawi, T.M., Ismail, A., Jenner, P., 2005. Age-associated changes in protein oxidation and proteasome activities in rat brain: modulation by antioxidants. Biochem. Biophys. Res. Commun. 336, 386–391.

Frick, K.M., Baxter, M.G., Markowska, A.L., Olton, D.S., Price, D.L., 1995. Age-related spatial reference and working memory deficits assessed in the water maze. Neurobiol. Aging 16, 149–160.

Frisina, R.D., Singh, A., Bak, M., Bozorg, S., Seth, R., Zhu, X., 2011. F1 (CBA× C57) mice show superior hearing in old age relative to their parental strains: Hybrid vigor or a new animal model for "Golden Ears"? Neurobiol. Aging 32, 1716–1724.

Frisina, R.D., Zhu, X., 2010. Auditory sensitivity and the outer hair cell system in the CBA mouse model of age-related hearing loss. Open Access Anim. Physiol. 2, 9.

Gallagher, M., Pelleymounter, M.A., 1988. Spatial learning deficits in old rats: a model for memory decline in the aged. Neurobiol. Aging 9, 549–556.

Gerich, F.J., Funke, F., Hildebrandt, B., Faßhauer, M., Müller, M., 2009. H2O2-mediated modulation of cytosolic signaling and organelle function in rat hippocampus. Pflügers Arch. 458, 937–952.

Gerich, F.J., Hepp, S., Probst, I., Müller, M., 2006. Mitochondrial inhibition prior to oxygen-withdrawal facilitates the occurrence of hypoxia-induced spreading depression in rat hippocampal slices. J. Neurophysiol. 96, 492–504.

Golomb, J., Kluger, A., de Leon, M.J., Ferris, S.H., Convit, A., Mittelman, M.S., Cohen, J., Rusinek, H., De Santi, S., George, A.E., 1994. Hippocampal formation size in normal human aging: a correlate of delayed secondary memory performance. Learn. Mem. 1, 45–54.

Goodrick, C., Ingram, D., Reynolds, M., Freeman, J., Cider, N., 1990. Effects of intermittent feeding upon body weight and lifespan in inbred mice: interaction of genotype and age. Mech. Ageing Dev. 55, 69–87.

Hedden, T., Gabrieli, J.D.E., 2004. Insights into the ageing mind: a view from cognitive neuroscience. Nat. Rev. Neurosci. 5, 87–96.

Henry, K.R., McGinn, M.D., Chole, R.A., 1980. Age-related auditory loss in the Mongolian gerbil. Arch. Otorhinolaryngol. 228, 233–238.

Holm, S., 1979. A simple sequentially rejective multiple test procedure. Scand. J. Stat. 6, 65–70.

Hu, D., Serrano, F., Oury, T.D., Klann, E., 2006. Aging-dependent alterations in synaptic plasticity and memory in mice that overexpress extracellular superoxide dismutase. J. Neurosci. 26, 3933–3941.

Huang, S., Heikal, A.A., Webb, W.W., 2002. Two-photon fluorescence spectroscopy and microscopy of NAD(P)H and flavoprotein. Biophys. J. 82, 2811–2825.

Huang, T.T., Leu, D., Zou, Y., 2015. Oxidative stress and redox regulation on hippocampal-dependent cognitive functions. Arch. Biochem. Biophys. 576, 2–7.

Husson, T.R., Issa, N.P., 2009. Functional imaging with mitochondrial flavoprotein autofluorescence: theory, practice, and applications. In: Frostig, R.D. (Ed.), In Vivo Optical Imaging of Brain Function. CRC Press, New York, pp. 221–253.

Jiang, H., Talaska, A.E., Schacht, J., Sha, S.-H., 2007. Oxidative imbalance in the aging inner ear. Neurobiol. Aging 28, 1605–1612.

Kudin, A.P., Kudina, T.A., Seyfried, J., Vielhaber, S., Beck, H., Elger, C.E., Kunz, W.S., 2002. Seizure-dependent modulation of mitochondrial oxidative phosphorylation in rat hippocampus. Eur. J. Neurosci. 15, 1105–1114.

Kunz, W.S., Gellerich, F.N., 1993. Quantification of the content of fluorescent flavoproteins in mitochondria from liver, kidney cortex, skeletal muscle, and brain. Biochem. Med. Metab. Biol. 50, 103–110.

Levine, B., Svoboda, E., Hay, J.F., Winocur, G., Moscovitch, M., 2002. Aging and autobiographical memory: dissociating episodic from semantic retrieval. Psychol. Aging 17, 677.

Lin, F.R., Ferrucci, L., Metter, E.J., An, Y., Zonderman, A.B., Resnick, S.M., 2011a. Hearing loss and cognition in the Baltimore Longitudinal Study of Aging. Neuropsychology 25, 763.

Lin, F.R., Metter, E.J., O'Brien, R.J., Resnick, S.M., Zonderman, A.B., Ferrucci, L., 2011b. Hearing loss and incident dementia. Arch. Neurol. 68, 214–220.

Ling, L., Hughes, L., Caspary, D., 2005. Age-related loss of the GABA synthetic enzyme glutamic acid decarboxylase in rat primary auditory cortex. Neuroscience 132, 1103–1113.

Llano, D.A., Slater, B.J., Lesicko, A.M., Stebbings, K.A., 2014. An auditory colliculo-thalamocortical brain slice preparation in mouse. J. Neurophysiol. 111, 197–207.

Llano, D.A., Turner, J., Caspary, D.M., 2012. Diminished cortical inhibition in an aging mouse model of chronic tinnitus. J. Neurosci. 32, 16141–16148.

Lores-Arnaiz, S., Perazzo, J.C., Prestifilippo, J.P., Lago, N., D'Amico, G., Czerniczyniec, A., Bustamante, J., Boveris, A., Lemberg, A., 2005. Hippocampal mitochondrial dysfunction with decreased mtNOS activity in prehepatic portal hypertensive rats. Neurochem. Int. 47, 362–368.

Maguire, E.A., Frith, C.D., 2003. Aging affects the engagement of the hippocampus during autobiographical memory retrieval. Brain 126, 1511–1523.

Maleki, S., Sepehr, R., Staniszewski, K., Sheibani, N., Sorenson, C.M., Ranji, M., 2012. Mitochondrial redox studies of oxidative stress in kidneys from diabetic mice. Biomed. Opt. Express 3, 273–281.

Manczak, M., Jung, Y., Park, B.S., Partovi, D., Reddy, P.H., 2005. Time-course of mitochondrial gene expressions in mice brains: implications for mitochondrial dysfunction, oxidative damage, and cytochrome c in aging. J. Neurochem. 92, 494–504.

Mayevsky, A., 1984. Brain NADH redox state monitored in vivo by fiber optic surface fluorometry. Brain Res. Rev. 7, 49–68.

Mendelson, J., Ricketts, C., 2001. Age-related temporal processing speed deterioration in auditory cortex. Hear. Res. 158, 84–94.

Miller, R.A., Harper, J.M., Galecki, A., Burke, D.T., 2002. Big mice die young: early life body weight predicts longevity in genetically heterogeneous mice. Aging Cell 1, 22–29.

Moscicki, E.K., Elkins, E.F., Baurn, H.M., McNarnara, P.M., 1985. Hearing Loss in the Elderly: An Epidemiologic Study of the Framingham Heart Study Cohort. Ear Hear. 6, 184–190.

Navarro, A., López-Cepero, J.M., Bández, M.J., Sanchez-Pino, M.-J., Gómez, C., Cadenas, E., Boveris, A., 2008. Hippocampal mitochondrial dysfunction in rat aging. Am. J. Physiol. Regul. Integr. Comp. Physiol. 294, R501–R509.

O'Brien, R.M., 2007. A caution regarding rules of thumb for variance inflation factors. Qual. Quant. 41, 673–690.

Ohlemiller, K.K., Dahl, A.R., Gagnon, P.M., 2010. Divergent aging characteristics in CBA/J and CBA/CaJ mouse cochleae. J. Assoc. Res. Otolaryngol. 11, 605–623.

Parihar, M.S., Brewer, G.J., 2007. Simultaneous age-related depolarization of mitochondrial membrane potential and increased mitochondrial reactive oxygen species production correlate with age-related glutamate excitotoxicity in rat hippocampal neurons. J. Neurosci. Res. 85, 1018–1032.

Parihar, M.S., Kunz, E.A., Brewer, G.J., 2008. Age-related decreases in NAD (P) H and glutathione cause redox declines before ATP loss during glutamate treatment of hippocampal neurons. J. Neurosci. Res. 86, 2339—2352.

Parthasarathy, A., Cunningham, P.A., Bartlett, E.L., 2010. Age-related differences in auditory processing as assessed by amplitude-modulation following responses in quiet and in noise. Front. Aging Neurosci. 2, 152.

Paula-Lima, A.C., Adasme, T., Hidalgo, C., 2014. Contribution of Ca2+ release channels to hippocampal synaptic plasticity and spatial memory: potential redox modulation. Antioxid. Redox Signal. 21, 892—914.

Persson, J., Nyberg, L., Lind, J., Larsson, A., Nilsson, L.-G., Ingvar, M., Buckner, R.L., 2006. Structure—function correlates of cognitive decline in aging. Cereb. Cortex 16, 907—915.

Piantanelli, L., Zaia, A., Rossolini, G., Piantanelli, A., Basso, A., Anisimov, V.N., 2001. Long-live euthymic BALB/c-nu mice. I. Survival study suggests body weight as a life span predictor. Mech. Ageing Dev. 122, 463—475.

Poirrier, A.L., Pincemail, J., Van Den Ackerveken, P., Lefebvre, P.P., Malgrange, B., 2010. Oxidative stress in the cochlea: an update. Curr. Med. Chem. 17, 3591—3604.

Ranji, M., Matsubara, M., Leshnower, B.G., Hinmon, R.H., Jaggard, D.L., Chance, B., Gorman, R.C., Gorman, J.H., 2009. Quantifying acute myocardial injury using ratiometric fluorometry. Biomed. Eng. IEEE Trans. 56, 1556—1563.

Reinert, K.C., Gao, W., Chen, G., Ebner, T.J., 2007. Flavoprotein autofluorescence imaging in the cerebellar cortex in vivo. J. Neurosci. Res. 85, 3221—3232.

Rodrigues Siqueira, I., Fochesatto, C., da Silva Torres, I.L., Dalmaz, C., Alexandre Netto, C., 2005. Aging affects oxidative state in hippocampus, hypothalamus and adrenal glands of Wistar rats. Life Sci. 78, 271—278.

Salehpour, F., Ghanian, Z., Yang, C., Zheleznova, N.N., Kurth, T., Dash, R.K., Cowley, A.W., Ranji, M., 2015. Effects of p67phox on the mitochondrial oxidative state in the kidney of Dahl salt-sensitive rats: optical fluorescence 3-D cry- oimaging. Am. J. Physiol. Renal Physiol. 309, F377—F382.

Samorajski, T., Delaney, C., Durham, L., Ordy, J., Johnson, J., Dunlap, W., 1985. Effect of exercise on longevity, body weight, locomotor performance, and passive- avoidance memory of C57BL/6J mice. Neurobiol. Aging 6, 17—24.

Sepehr, R., Staniszewski, K., Maleki, S., Jacobs, E.R., Audi, S., Ranji, M., 2012. Optical imaging of tissue mitochondrial redox state in intact rat lungs in two models of pulmonary oxidative stress. J. Biomed. Opt. 17, 046010.

Serrano, F., Klann, E., 2004. Reactive oxygen species and synaptic plasticity in the aging hippocampus. Ageing Res. Rev. 3, 431—443.

Simpson, G.V., Knight, R.T., Brailowsky, S., Prospero-Garcia, O., Scabini, D., 1985. Altered peripheral and brainstem auditory function in aged rats. Brain Res. 348, 28—35.

Siqueira, I.R., Fochesatto, C., da Silva Torres, I.L., Dalmaz, C., Netto, C.A., 2005. Aging affects oxidative state in hippocampus, hypothalamus and adrenal glands of Wistar rats. Life Sci. 78, 271—278.

Sohal, R.S., Weindruch, R., 1996. Oxidative stress, caloric restriction, and aging. Science 273, 59—63.

Someya, S., Yamasoba, T., Weindruch, R., Prolla, T.A., Tanokura, M., 2007. Caloric restriction suppresses apoptotic cell death in intact mammalian cochlea and leads to prevention of presbycusis. Neurobiol. Aging 28, 1613—1622.

Staecker, H., Zheng, Q.Y., Van De Water, T.R., 2001. Oxidative stress in aging in the C57B16/J mouse cochlea. Acta Otolaryngol. 121, 666—672.

Stebbings, K., Choi, H., Ravindra, A., Caspary, D., Turner, J., Llano, D., 2016. Ageing- related changes in GABAergic inhibition in mouse auditory cortex, measured using in vitro flavoprotein autofluorescence imaging. J. Physiol. 594, 207—221.

Syka, J., 2010. The Fischer 344 rat as a model of presbycusis. Hear. Res. 264, 70—78.

Takesian, A.E., Kotak, V.C., Sanes, D.H., 2012. Age-dependent effect of hearing loss on cortical inhibitory synapse function. J. Neurophysiol. 107, 937—947.

Walton, J.P., Frisina, R.D., O'Neill, W.E., 1998. Age-related alteration in processing of temporal sound features in the auditory midbrain of the CBA mouse. J. Neurosci. 18, 2764—2776.

White, R., Wittenberg, B., 1993. NADH fluorescence of isolated ventricular myocytes: effects of pacing, myoglobin, and oxygen supply. Biophys. J. 65, 196.

Wong-Riley, M.T., 1989. Cytochrome oxidase: an endogenous metabolic marker for neuronal activity. Trends Neurosci. 12, 94—101.

Yamasoba, T., Someya, S., Yamada, C., Weindruch, R., Prolla, T.A., Tanokura, M., 2007. Role of mitochondrial dysfunction and mitochondrial DNA mutations in age- related hearing loss. Hear. Res. 226, 185—193.